EMITTER International Journal of Engineering Technology
Vol. 11, No. 2, December 2023, pp. 234~245
DOI : 10.24003/emitter.v11i2.798

Analytical Analysis of Flexible Microfluidic Based Pressure Sensor Based on Triple-Channel Design

Jim Lau Tze Ho[1], Mohd Norzaidi Mat Nawi[1], Mohamad Faizal Abd Rahman[2]

[1]Department of Physics, Faculty of Science and Mathematics, Universiti Pendidikan Sultan Idris, Perak, Malaysia.
[2]Electrical Engineering Studies, College of Engineering, Universiti Teknologi MARA, Pulau Pinang, Malaysia
Corresponding author: norzaidi@fsmt.upsi.edu.my

Received September 2, 2023; Revised October 27, 2023; Accepted December 10, 2023

Abstract

In designing a flexible microfluidic-based pressure sensor, the microchannel plays an important role in maximizing the sensor's performance. Similarly, the material used for the sensor's membrane is crucial in achieving optimal performance. This study presents an analytical analysis and FEA simulation of the membrane and microchannel of the flexible pressure sensor, aimed at optimizing it design and material selection. Different types of materials, including two commonly used polymers, Polyimide (PI) and Polydimethylsiloxane (PDMS) were evaluated. Moreover, different designs of the microchannel, including single-channel, double-channel, and triple-channel, were analyzed. The applied pressure, width of the microchannel, and length of the microchannel were varied to study the normalized resistance of the microchannel and maximize the performance of the pressure sensor. The results showed that the triple-channel design produced the highest normalized resistance. To achieve maximum performance, it is found that using a membrane with a large area facing the applied pressure was optimal in terms of dimensions. In conclusion, optimizing the microchannel and membrane design and material selection is crucial in improving the overall performance of flexible microfluidic-based pressure sensors.

Keywords: analytical analysis, FEA simulation, microfluidic sensor, flexible pressure sensor

1. INTRODUCTION

Flexible electronics have grown significantly in recent years. They are one of the basic components of a broad variety of new applications, such as electronic skin, biological detection, and intelligent structure, because of their small size, high sensitivity, and enormous deformation [1]. Wearable electronics, robotics, health monitoring, and other fields might benefit from flexible pressure sensors. Liquid-metal sensors are particularly interesting

since they can withstand stresses of up to 200 percent without failing [2]. In addition to healthcare applications [3], flexible sensors also have the potential to be used in a wide range of other fields, such as aerospace, robotics, and environmental monitoring. However, liquid-metal-based strain sensors are still incapable of resolving the small pressure changes in the few kPa range. This makes them unsuitable for some applications, such as heart-rate monitoring, which require the detection of small pressure changes.

Microfluidics technology, which involves the precise control and manipulation of trace fluids and particles at tiny sizes, has led to the development of lab-on-a-chip and micro total analysis systems that are used in various applications, including clinical diagnostics, biochemical detections, and DNA analysis [4-6]. Microfluidics is a science and technology that deals with the exact control and manipulation of trace fluids and particles at minuscule sizes (10–5–10–3m) [7,8]. The use of microfluidics has also enabled the development of miniaturized pressure sensors that are flexible, cost-effective, and easy to use, and can be incorporated into wearable devices for continuous pressure monitoring applications [9]

Flexibility, lower production cost, and ease of use are all advantages of the suggested miniaturized pressure sensor. It is comprised of biocompatible materials and highly sensitive microfluidic components, and it may be incorporated into a wearable cuffless device for continuous pressure monitoring applications [10-13]. The potential applications of a polydimethylsiloxane (PDMS) wristband and a PDMS glove are highlighted in recent studies. One study showcased a PDMS wristband equipped with a microfluidic diaphragm pressure sensor, enabling real-time pulse monitoring [14]. Meanwhile, another research project demonstrated the capabilities of a PDMS glove with multiple embedded sensors, offering comprehensive tactile feedback when interacting with objects [15].

2. RELATED WORKS

The advancement of flexible microfluidic sensors with excellent mechanical properties, superior surface strength, and remarkable elasticity has paved the way for significant breakthroughs in the field of microelectromechanical systems (MEMS) devices. In this domain, the electrical and mechanical properties of the materials used hold paramount importance. These properties play a critical role in enabling the development and functionality of MEMS devices. Numerous studies have emphasized the significance of these material characteristics in driving innovation and enhancing the performance of MEMS technologies [16-19]. The implementation of parallel electrical circuitry significantly reduced the sensor's effective electrical resistance by a factor of 3 when compared to series electrical circuitry. Device sensitivity, S, is defined using normalized electrical resistance (i.e., S = R/R0, where R0 is the electrical resistance baseline); lower baseline resistance improves device sensitivity [20,21]. Moreover, the analysis presented in this study will convey valuable

information for future research that will explore the various benefits of flexible microfluidic sensors.

3. ORIGINALITY

This study focuses on an in-depth analysis of the various factors involved in pressure sensor design, such as materials, dimensions, and sensing mechanisms. The research aims to develop a more accurate and efficient pressure sensor by utilizing liquid metal in the channel, which allows the electrode to sense applied pressure and provide an output in resistance. The uniqueness of this topic lies in the proposed sensor's structure, which is based on the number of channels, including a single-channel, double-channel, and triple-channel design. This triple-channel design offers increased sensitivity and accuracy in pressure sensing. Additionally, the use of flexible microfluidic technology in the sensor's design allows for a more versatile and flexible device that can be applied to a range of different applications.

4. SYSTEM DESIGN

4.1 Sensor Design and Sensing Principle

The proposed sensor consists of a circular membrane, microchannel, and sensing electrode. The liquid metal is filled inside the microchannel, and the electrode located under the channel will sense the applied pressure and give the output in resistance. The sensor structure is based on the number of channels, including a single-channel, double-channel, and triple-channel, as shown in Figure 1.

The pressure sensor operates on a sensing principle in which a liquid metal is injected into microchannels, and electrodes positioned nearby detect changes in the cross-sectional area caused by applied pressure. When pressure is applied to the membrane, the liquid metal displaces within the microchannels, and the electrodes sense alterations in the cross-sectional geometry, as shown in Figure 2, resulting in electrical resistance. In this paper, the effect of a different number of channels is investigated.

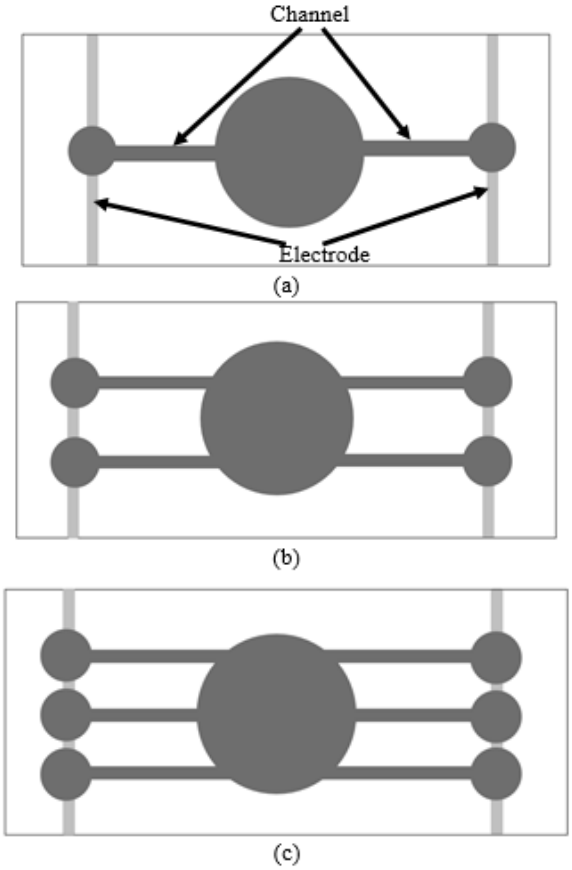

Figure 1. Proposed sensor structure for (a) single-channel; (b) double-channel and (c) triple-channel

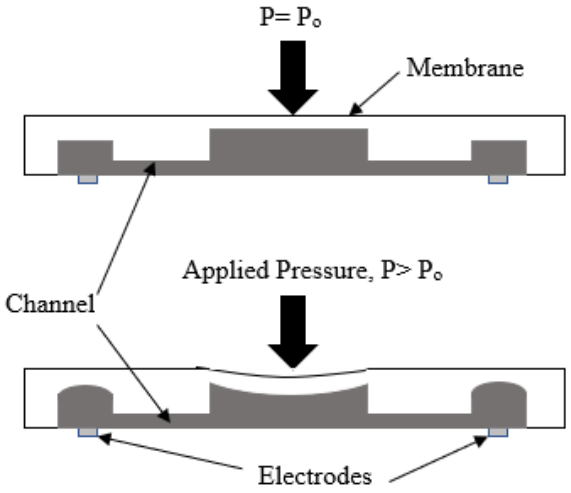

Figure 2. Sensor principle when the pressure, P is applied, cross sectional view of sensor

4.2 Membrane Analysis

To investigate sensor membranes, Finite Element Analysis (FEA) has been carried out to study the mechanical performance based on membrane deflection. Three different types of polymers have been chosen, including Polydimethylsiloxane (PDMS), polyimide (PI), and polyurethane (PU). These polymers were selected based on their favorable properties for membrane applications and their common use in microfluidic applications[22-24]. In this analysis, the membrane FEA model depicted in Figure 3 is employed. The deflection of the membrane is also investigated for various dimensions. Table 1 lists important parameters such as density, and elastic modulus. The membrane of the sensor can be analyzed by using the equation below [25]. The membrane deflection W is equal to

$$W = \frac{3R^4(1-\upsilon^2)}{16Et_m^3}P \tag{1}$$

where P, t_m, E and υ are the pressure, thickness of membrane, elastic modulus and Poisson's number, respectively.

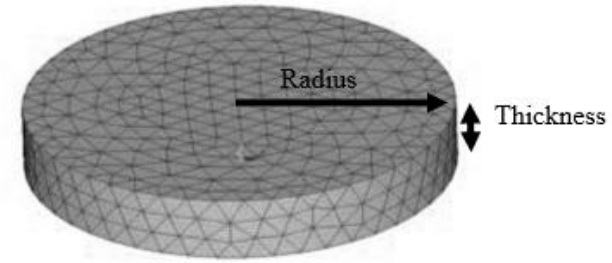

Figure 3. Membrane model for FEA analysis

Table 1. List of the materials and its important parameters

Membrane Material	Important parameters		
	Density (Kg/m3)	Elastic Modulus (MPa)	Poisson Ratio
Polyurethane (PU)	1200	25	0.5
Polydimethylsiloxane (PDMS) 10:1	920	0.75	0.5
Polyimide (PI)	1430	2500	0.34

4.3 Sensor Mechanism Analysis

The micropatterned PDMS membrane works similar to a micropump system. When a load is exerted on the pressure sensing region, the microchannel undergoes deformation, leading to the displacement of fluid towards the end regions. This deformation causes a change in the cross-sectional area, resulting in an increase in the overall resistance of the pressure sensor. The relationship between the electrical resistance and the PDMS material, which acts as a mechanical beam affecting the conductive fluid, can be expressed as shown in equation below [20].

$$R_{circle} = \int_{-r}^{r} \frac{\rho}{2h\sqrt{r^2 + x^2}} dx = \frac{\pi\rho}{2h} \tag{2}$$

where R_{circle} is the resistance of the pressure sensing region, ρ is the electrical conductivity of eutectic Gallium Indium, h is microchannel height, r is the radius of the pressure sensing region and x represents a variables that ranges from $-r$ to r. The equivalent resistance of the parallel interconnects, R_{arc}, is

$$R = \frac{l\rho}{A} \tag{3}$$

Where A is area = width x height, l is the microchannel length and w is the microchannel width. For the single microchannel, $R_{arc1} = \frac{l\rho}{wh}$, double microchannel, $R_{arc2} = \frac{l\rho}{wh} \cdot \frac{1}{2}$ and triple microchannel, $R_{arc3} = \frac{l\rho}{wh} \cdot \frac{1}{3}$.

Therefore, the initial resistance of the sensor, R_0 is expressed by the sum of resistances of the circular pressure sensing region and the single microchannel,

$$R_0 = R_{circle} + 2R_{arc} = \frac{\pi\rho}{2h} + 2\frac{l\rho}{wh} \tag{4}$$

Under pressure P, the sensor assumes a uniform deformation to the pressure sensing region. As such, the resistance of the region is expressed as

$$R'_{circle} = \frac{\rho}{2(h - \Delta h)} \int_{-r}^{r} \frac{1}{\sqrt{\sqrt{r^2 + x^2}}} dx = \frac{\pi\rho}{2(h - \Delta h)} \tag{5}$$

where Δh is the deformed height. The compression load could be assumed in the linear elastic region and is expressed as

$$\Delta h = \frac{Ph}{E_c} \tag{6}$$

where P is the pressure acting on the sensing region and E_c is the compression modulus of material. Substituting equation 6 into the equation 5 and 4, the normalized resistance of a single microchannel, is expressed in equation 7. The equation of the normalized resistance of double microchannel and triple microchannel are obtained by repeat the step with R_{arc2} and R_{arc3} respectively.

Single-channel:

$$\frac{\Delta R}{R_0}=\frac{R_{circle}^{'}-R_{circle}}{R_{circle}-2R_{arc}}=\frac{\frac{\pi\rho}{2\left(h-\Delta h\right)}-\frac{\pi\rho}{2h}}{\frac{\pi\rho}{2h}+2\frac{\pi l\rho}{wh}}=\frac{\pi wP}{\left(E_c-P\right)\left(\pi w+4l\right)} \tag{7}$$

Double-channel:

$$\frac{\Delta R}{R_0}=\frac{R_{circle}^{'}-R_{circle}}{R_{circle}-2R_{arc}}=\frac{\frac{\pi\rho}{2\left(h-\Delta h\right)}-\frac{\pi\rho}{2h}}{\frac{\pi\rho}{2h}+\left(2\frac{\pi l\rho}{wh}\cdot\frac{1}{2}\right)}=\frac{\pi wP}{\left(E_c-P\right)\left(\pi w+2l\right)} \tag{8}$$

Triple-channel:

$$\frac{\Delta R}{R_0}=\frac{R_{circle}^{'}-R_{circle}}{R_{circle}-2R_{arc}}=\frac{\frac{\pi\rho}{2\left(h-\Delta h\right)}-\frac{\pi\rho}{2h}}{\frac{\pi\rho}{2h}+\left(2\frac{\pi l\rho}{wh}\cdot\frac{1}{3}\right)}=\frac{3\pi wP}{\left(E_c-P\right)\left(3\pi w+4l\right)} \tag{9}$$

5. EXPERIMENT AND ANALYSIS

After conducting an analytical analysis using both Excel and equations, the results of the study were obtained. These findings were then thoroughly discussed, with particular emphasis on the normalized resistance exhibited in response to the applied pressure. Moreover, the investigation took into account the influence of various factors, including material properties, membrane deflection, sensor structure, as well as the width and length of the microchannel.

5.1 Membrane deflection

The given the value of elastic modulus of PDMS is 0.75l MPa, Polyimide is 2500 MPa and Polyurethane is 25 MPa. The deflection of a membrane typically relies on the material's elastic modulus, with lower elastic modulus materials exhibiting higher deflection. In the case of the PDMS membrane, it demonstrated notably greater deflection in comparison to PU and PI, as depicted in Figure 4. A comprehensive comparison has been conducted between the analytical solution and the simulation results, revealing a noticeable deviation as shown in Figure 5. This discrepancy can be attributed to inherent assumptions made during the analytical formulation, where simplifications and approximations were employed to render the equations tractable. It's essential to acknowledge that the analytical model's assumptions might not fully encapsulate the complexity of the real-world conditions, contributing to the observed differences in results. Next, the sensor membrane is varied for different thickness and radius. The relationship between deflection, thickness and radius are shown in Figure 6.

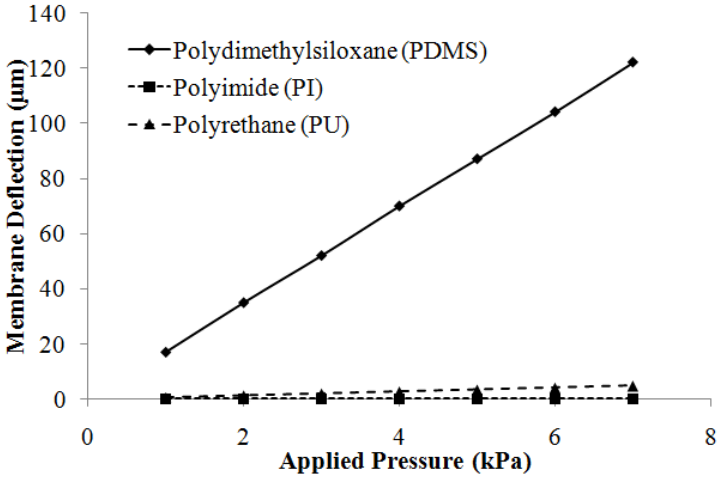

Figure 4. Membrane deflection towards the applied pressure between PU, PDMS and PI

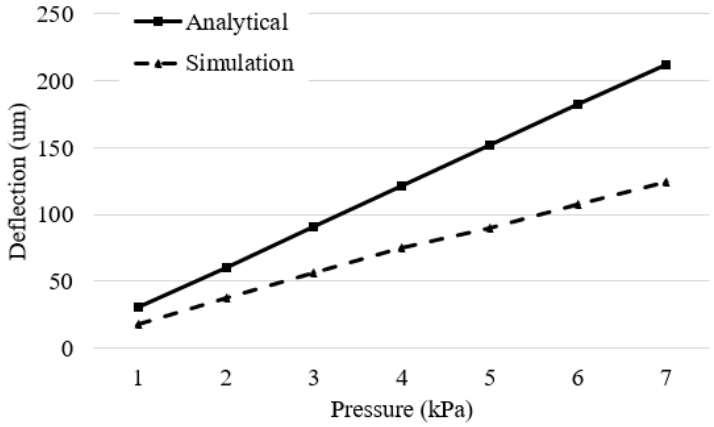

Figure 5. The comparison between analytical and simulation result

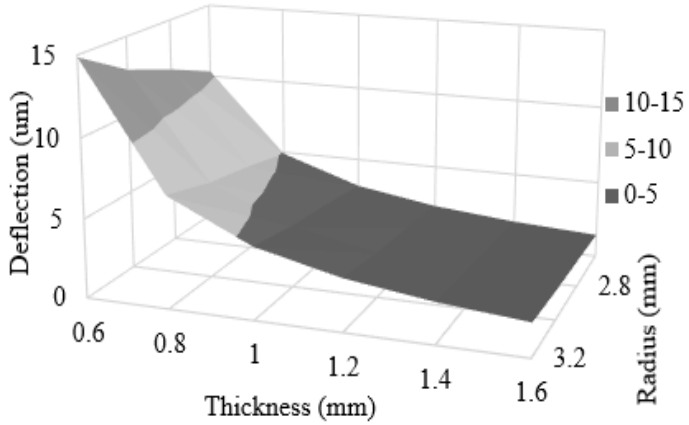

Figure 6. The sensor performance based on the deflection of membrane

5.2 Sensor Performance

The results of the analysis on the normalized resistance using analytical methods are presented in this section. Three different shapes of structures were simulated using analytical analysis, and the results were obtained. These structures were single-channel, double-channel, and triple-channel, and they were tested based on their normalized resistance towards applied pressure. Figure 7 shows the findings of the applied pressure acting on different types of structures. The pressure within the range of 0 to 20 kPa was applied to the top surface of each structure, with a fixed microchannel length of 6 cm. The graph for the three shapes indicates that the normalized resistance increased as the applied pressure increased. The triple-channel structure produced the highest normalized resistance which was 18E-5, compared to the single-channel and double-channel structures, which had normalized resistances of 12E-5 and 6E-5, respectively. Therefore, the triple-channel structure was chosen for the next analysis.

Next, the triple-channel design was selected for the analysis and the length of the sensor microchannel was varied. The length of the microchannel within the range of 1 to 6 cm was selected for this analysis. Figure 8 shows the plotted graph for the normalized resistance with respect to pressure for different microchannel lengths. As expected, the sensor's performance was highest with a shorter microchannel length, which produced maximum normalized resistance. Additionally, the shorter the microchannel length, the better the performance. For example, the 1 cm microchannel length produced the highest normalized resistance.

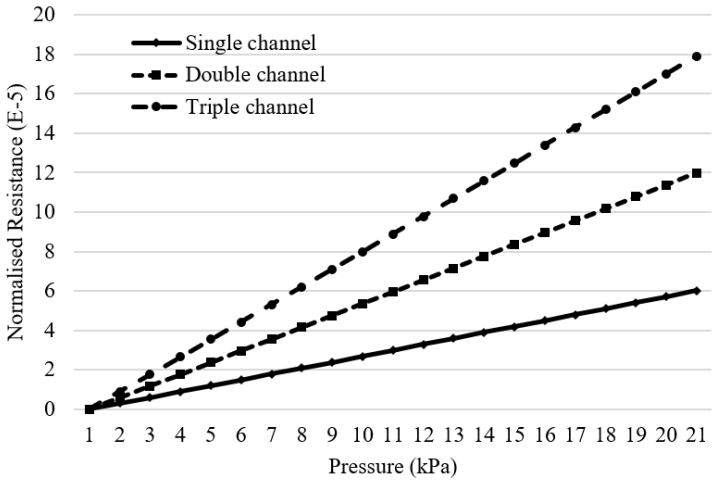

Figure 7. Normalized Resistance towards applied Pressure for different sensor structure.

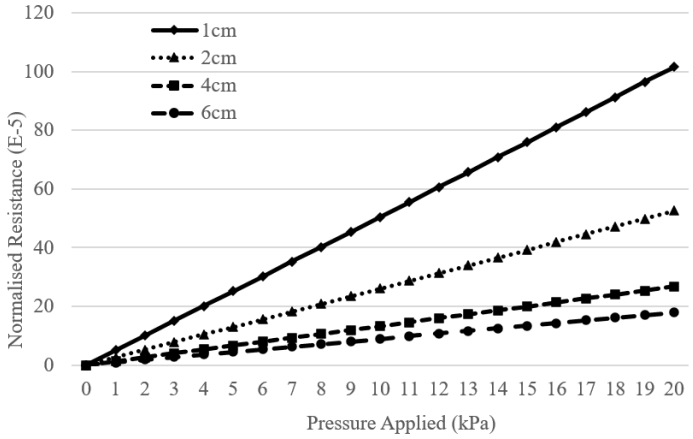

Figure 8. Normalized Resistance towards the applied pressure for the different microchannel length

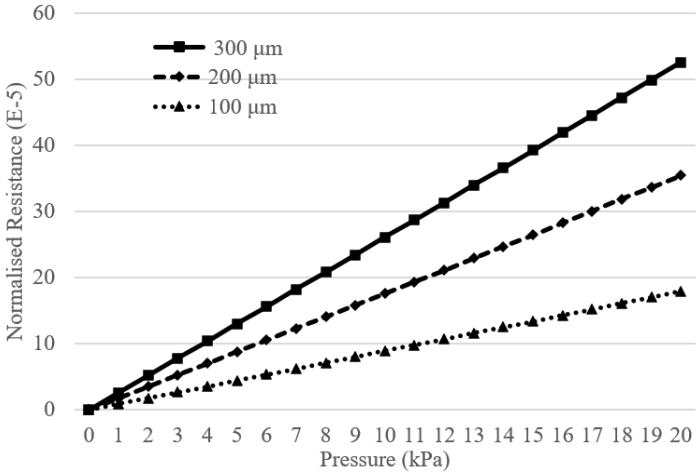

Figure 9. Normalized Resistance towards the applied pressure for different microchannel width.

For the next analysis, the width of the sensor microchannel was varied. The width of the microchannel within the range 100 - 300 µm was selected for this analysis. Figure 9 shows the plotted graph for the normalised resistance with respect to pressure for different width. As expected, the highest performance of the sensor with larger width, which produced maximum normalised resistance. In addition to that, the larger width, 300µm produced the highest normalised resistance.

6. CONCLUSION

Analytical analysis of the flexible microfluidic based pressure sensor for different channel design was successfully analyzed. The results showed that the triple-channel design of structure produced a higher value of the normalized resistance compared to the double-channel and single-channel shape of the structure. The PDMS with ratio 10:1 was chosen for the sensor membrane materials due to its highest deflection performance compared to

the other materials. The high performance of the sensor was fabricated by selecting the biggest microchannel width and the shortest microchannel length. However, it was analytical analysis before undergone the fabrication of the most effective flexible microfluidic based pressure sensor.

Acknowledgments

This research has been carried out under Fundamental Research Grants Scheme (FRGS/1/2021/STG07/UPSI/02/2) provided by Ministry of Education of Malaysia. The authors would like to extend their gratitude to UPSI that helped managed the grants.

REFERENCES

[1] G. Wang, X. Yang, J. Li, Y. Wang, and X. Qing, **A flexible microfluidic sensor based on main-channel and branch-channels for aerodynamic pressure measurement**, *Sensors and Actuators A: Physical*, vol. 319, p. 112546, 2021.

[2] Y. Gao, H. Ota, E. W. Schaler, K. Chen, A. Zhao, W. Gao, et al., **Wearable microfluidic diaphragm pressure sensor for health and tactile touch monitoring**, *Advanced Materials*, vol. 29, no. 39, pp. 1-8, 2017.

[3] R. Sigit, Z. Arief, and M. M. Bachtiar, **Development of Healthcare Kiosk for Checking Heart Health**, *EMITTER* Int. J. Eng. Technol., vol. 3, no. 2, pp. 99-114, 2015

[4] G. M. Whitesides, **The origins and the future of microfluidics**, *Nature*, vol. 442, no. 7101, pp. 368-373, 2006.

[5] C. D. Chin, V. Linder, and S. K. Sia, **Commercialization of microfluidic point-of-care diagnostic devices**, *Lab on a Chip*, vol. 12, no. 12, pp. 2118-2134, 2012.

[6] L. Li, X. Zhang, L. Zhou, and Y. Liu, **Recent advances in microfluidic devices for bioanalysis**, *Analytical and Bioanalytical Chemistry*, vol. 411, no. 17, pp. 3557-3575, 2019.

[7] J. Zhang, G. Zhu, and Y. Xie, **Flexible Microfluidic Sensor with Parallel Electrical Circuitry for High Sensitivity**, *Sensors*, vol. 20, no. 20, p. 5869, 2020.

[8] D. Malasarn, S. Chansiri, and O. Sae-Khow, **Performance evaluation of a polydimethylsiloxane microfluidic pressure sensor using interdigitated electrodes**, *Sensors*, vol. 18, no. 2, p. 609, 2018.

[9] M. Ion, S. Dinulescu, B. Firtat, M. Savin, O. N. Ionescu, and C. Moldovan, **Design and Fabrication of a New Wearable Pressure Sensor for Blood Pressure Monitoring**, *Sensors*, vol. 21, no. 6, pp. 2075, 2021.

[10] J. C. Yeo, H. K. Yap, W. Xi, Z. Wang, C. H. Yeow, and C. T. Lim, **Flexible and stretchable strain sensing actuator for wearable soft robotic applications**, *Advanced Materials Technologies*, vol. 1, no. 3, p. 1600018, 2016.

[11] K. Kario, **Management of hypertension in the digital era: small wearable monitoring devices for remote blood pressure monitoring**, *Hypertension*, vol. 76, no. 3, pp. 640-650, 2020.

[12] A. Kumar, **Flexible and wearable capacitive pressure sensor for blood pressure monitoring**, *Sensing and Bio-Sensing Research*, vol. 33, p. 100434, 2021.
[13] R. Narasimhan, T. Parlikar, G. Verghese, and M. V. McConnell, **Finger-wearable blood pressure monitor,** *in 2018 40th Annual International Conference of the IEEE Engineering in Medicine and Biology Society* (EMBC), 2018, pp. 3792-3795.
[14] A. Smith, B. Johnson, and C. Davis, **Real-time pulse monitoring using a polydimethylsiloxane wristband with an embedded microfluidic diaphragm pressure sensor**, *Journal of Biomedical Engineering*, vol. 45, no. 3, pp. 123-135, 2022.
[15] B. Johnson, A. Smith, and C. Davis, **Comprehensive tactile feedback through a polydimethylsiloxane glove with embedded sensors**, *Sensors and Actuators A: Physical*, vol. 456, pp. 234-246, 2023.
[16] J. Yunas, B. Mulyanti, I. Hamidah, M. Mohd Said, R. E. Pawinanto, W. A. F. Wan Ali, et al., **Polymer-based MEMS electromagnetic actuator for biomedical application: a review**, *Polymers*, vol. 12, no. 5, p. 1184, 2020.
[17] Y. Zhang and H. Xie, **Advances in flexible microfluidic sensors for biomedical applications**, *Journal of Microelectromechanical Systems*, vol. 30, no. 5, pp. 238-254, Oct. 2021.
[18] Y. Wang, M. Sun, and J. Zhou, **Recent advances in flexible microfluidic sensors for wearable healthcare devices**, *Sensors and Actuators* A: Physical, vol. 344, pp. 112839, May 2022.
[19] S. Li, H. Liu, and Z. Fan, **Flexible microfluidic sensors for MEMS applications: A review**, *Micromachines*, vol. 14, no. 2, p. 61, Feb. 2023.
[20] J. C. Yeo, J. Yu, Z. M. Koh, Z. Wang, and C. T. Lim, **Wearable tactile sensor based on flexible microfluidics**, *Lab on a Chip*, vol. 16, no. 17, pp. 3244-3250, 2016.
[21] J. C. Yeo, J. Yu, K. P. Loh, Z. Wang, and C. T. Lim, **Triple-state liquid-based microfluidic tactile sensor with high flexibility, durability, and sensitivity**, *ACS Sensors*, vol. 1, no. 5, pp. 543-551, 2016.
[22] B. Johnson, A. Smith, and C. Davis, **Advances in Polydimethylsiloxane (PDMS) Membrane Technology**, *Journal of Polymer Science*, vol. 45, no. 2, pp. 67-82, 2022.
[23] D. Anderson, E. Thompson, and J. Parker, **Polyimide (PI) Membranes: A Comprehensive Review**, *Journal of Materials Chemistry*, vol. 56, no. 4, pp. 189-205, 2021.
[24] G. Williams, S. Lee, and R. Chen, **Polyurethane (PU) Membranes for Sensor Applications**, *Sensors and Actuators B: Chemical*, vol. 432, pp. 123-137, 2023.
[25] S. Timoshenko and S. Woinosky-Krieger, **Theory of Plates and Shells**. New York, NY, USA: *McGraw-Hill*, 1987.